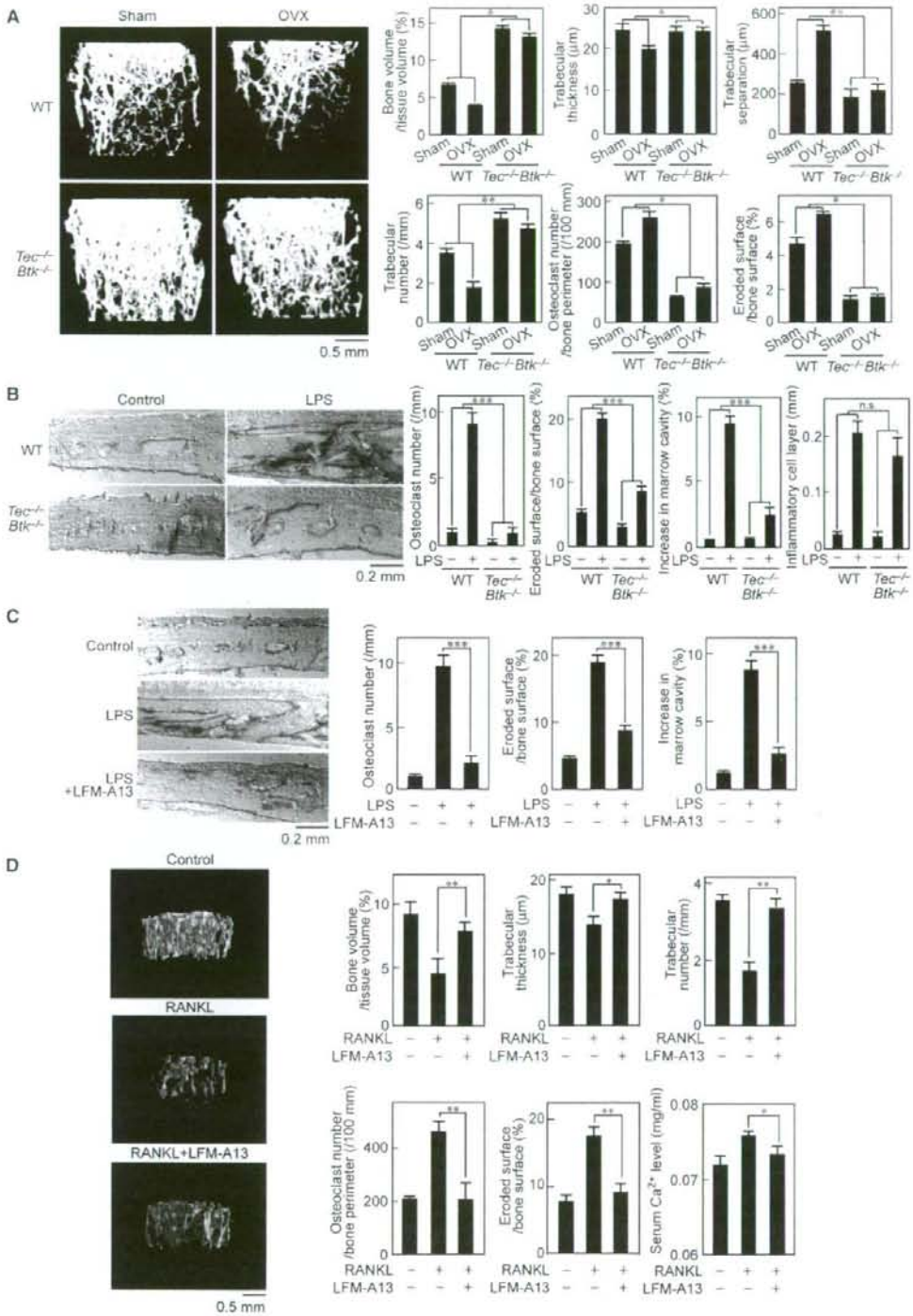
A
Sham
OVX
WT
Tec−/− Btk−/−
0.5 mm
Bone volume /tissue volume (%)
Trabecular thickness (μm)
Trabecular separation (μm)
Trabecular number (/mm)
Osteoclast number /bone perimeter (/100 mm)
Eroded surface /bone surface (%)
Sham OVX Sham OVX
WT Tec−/− Btk−/−
B
Control
LPS
WT
Tec−/− Btk−/−
0.2 mm
Osteoclast number (/mm)
Eroded surface/bone surface (%)
Increase in marrow cavity (%)
Inflammatory cell layer (mm)
n.s
LPS
WT Tec−/− Btk−/−
C
Control
LPS
LPS +LFM-A13
0.2 mm
Osteoclast number (/mm)
Eroded surface /bone surface (%)
Increase in marrow cavity (%)
LPS
LFM-A13
D
Control
RANKL
RANKL+LFM-A13
0.5 mm
Bone volume /tissue volume (%)
Trabecular thickness (μm)
Trabecular number (/mm)
Osteoclast number /bone perimeter (/100 mm)
Eroded surface /bone surface (%)
Serum Ca2+ level (mg/ml)
RANKL
LFM-A13

the rate of proliferation or apoptosis in *Blnk*$^{-/-}$*Lcp2*$^{-/-}$ BMMs was not significantly different from that in WT BMMs (Figure 5E). We found that in vitro osteoclast differentiation was severely abrogated in *Blnk*$^{-/-}$*Lcp2*$^{-/-}$ BMMs (Figure 5F), suggesting an important role for BLNK and SLP-76 in osteoclast differentiation. Thus, the scaffold proteins, with which the Tec kinases form a complex, have emerged as critical mediators of osteoclastogenic signals. These results further lend support to the crucial role of the RANKL-stimulated formation of the osteoclastogenic complex: the interaction of Tec kinases and their scaffold proteins results in the efficient phosphorylation of PLCγ.

Tec Kinases as Potential Therapeutic Targets for Bone Diseases

To investigate the role of Btk and Tec in the pathological activation of osteoclastogenesis, *Tec*$^{-/-}$*Btk*$^{-/-}$ mice were subjected to an ovariectomy (OVX)-induced model of postmenopausal osteoporosis (Aoki et al., 2006). The bone volume and trabecular bone number/connectivity were significantly reduced by the estrogen withdrawal in WT mice, but such a reduction was observed to a much lesser extent in *Tec*$^{-/-}$*Btk*$^{-/-}$ mice (Figure 6A and Figure S4). An increase in osteoclast number induced by OVX was also much lower in *Tec*$^{-/-}$*Btk*$^{-/-}$ mice (Figure 6A and Figure S4), suggesting a key role of Btk and Tec in the pathological activation of osteoclastogenesis.

Furthermore, *Tec*$^{-/-}$*Btk*$^{-/-}$ mice were subjected to a lipopolysaccharide (LPS)-induced model of inflammatory bone destruction (Takayanagi et al., 2000). *Tec*$^{-/-}$*Btk*$^{-/-}$ mice were protected from the activation of osteoclastogenesis and bone loss (Figure 6B), whereas the formation of an inflammatory cell layer, the number of infiltrated inflammatory cells, IKK activation, and serum levels of TNF-α and IL-6 in *Tec*$^{-/-}$*Btk*$^{-/-}$ mice were not different from those in WT mice (Figure 6B and Figure S5). These results prompted us to examine the therapeutic effects of Tec kinase inhibitor in disease models. Local administration of the Tec kinase inhibitor LFM-A13 had a marked therapeutic effect on the excessive osteoclast formation and bone destruction induced by LPS (Figure 6C) without affecting IKK activation or inflammatory cytokine levels in the serum (Figure S5), although it has been reported that Tec kinases are involved in the activation of immune cells, including lymphocytes and macrophages (Horwood et al., 2003; Mangla et al., 2004). These results suggest that the therapeutic effects of Tec kinase inhibitor in an LPS-induced model are not due to attenuated immune responses but rather are mainly caused by direct inhibitory effects on osteoclast precursor cells. It has been consistently reported that Btk is not essential for LPS-induced inflammatory cytokine production in macrophages under certain conditions (Hata et al., 1998; Perez de Diego et al., 2006).

To determine whether the Tec kinase inhibitor has therapeutic efficacy in a model of osteoporosis, we treated mice that were intraperitoneally injected with GST-RANKL. GST-RANKL injection resulted in an increase in osteoclast number and serum calcium concentration and a decrease in trabecular bone volume, but LFM-A13 treatment significantly ameliorated RANKL-induced bone loss (Figure 6D). These results demonstrate the inactivation of Tec family kinases to be a novel strategy for suppressing osteoclastogenesis in vivo.

DISCUSSION

RANKL-Induced Formation of the Osteoclastogenic Signaling Complex

An osteopetrotic phenotype in *Tec*$^{-/-}$*Btk*$^{-/-}$ mice revealed these two kinases to play a crucial role in the regulation of osteoclast differentiation. Btk and Tec are known to play a key role in proximal BCR signaling (Ellmeier et al., 2000), but this study establishes their crucial role in the integration of the two essential osteoclastogenic signals, RANK and ITAM (Figure 7). Thus, although immune and bone cells share components of signaling cascades, they play distinct roles in each cell type. Furthermore, this study identified an osteoclastogenic signaling complex composed of Tec kinases and adaptor proteins that may provide a new paradigm for the signal transduction mechanism of osteoclast differentiation: ITAM phosphorylation results in the recruitment of Syk, which phosphorylates adaptor proteins such as BLNK and SLP-76, which in turn function as scaffolds to recruit the Tec kinases activated by RANK and PLCγ to the osteoclast signaling complex so as to induce maximal calcium influx.

Such complexes are similar to those formed in the immunological synapse in T cells, which are associated with membrane rafts (Cherukuri et al., 2001). It has been reported that RANK accumulates in membrane rafts, and these specialized domains may play an important role in the RANK signal transduction (Ha et al., 2003). We observed that DAP12, Btk, BLNK, and PLCγ, as well as RANK, were recruited to caveolin-rich membrane domains, which are the crucial signaling domains contained in lipid rafts, after RANKL stimulation (Figure S6). Thus, it is likely that the complex containing both the RANK and ITAM signaling pathways is generated by RANKL stimulation and contributes to the facilitation of the osteoclastogenic signal transduction.

Linkage between Primary Immunodeficiency and Bone Homeostasis

The mutation of *Btk* in humans causes XLA, which is characterized by an arrest in B cell development and immunodeficiency

Figure 6. Tec Kinases as Potential Therapeutic Targets in Bone Diseases

(A) OVX-induced bone loss in WT and *Tec*$^{-/-}$*Btk*$^{-/-}$ mice (evaluated in the femurs and tibiae 3 weeks after sham operation or OVX). The trabecular thickness, separation, and number were obtained from three-dimensional microstructural analysis by microcomputed tomography. Bone volume, osteoclast number, and eroded surface were based on the bone morphometric analysis.

(B) Inflammation-induced bone destruction in WT and *Tec*$^{-/-}$*Btk*$^{-/-}$ mice. Histology of the calvarial bone injected with saline (control) or LPS in WT and *Tec*$^{-/-}$*Btk*$^{-/-}$ mice (TRAP and hematoxylin staining).

(C) Effect of local administration of the Tec kinase inhibitor LFM-A13 (20 mg/kg) on LPS-induced osteoclast formation and bone destruction (TRAP and hematoxylin staining). This inhibitor at this dosage had marginal effects on B cells.

(D) Effect of local administration of LFM-A13 (20 mg/kg) on RANKL-induced osteoclast formation and bone loss. After mice were sacrificed 1.5 hr after the final injection, serum calcium level was measured, and three-dimensional microstructural analysis (femur) and the bone morphometric analysis (tibia) were performed.

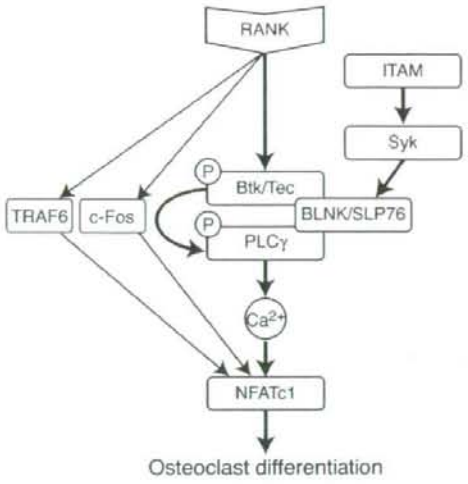

Figure 7. Integration of the RANK and ITAM Signals by Tec Kinases
RANKL binding to RANK results in activation of classical pathways involving TRAF6 and c-Fos. In addition, Tec kinases are phosphorylated by RANK. ITAM phosphorylation results in the recruitment of Syk, leading to activation of adaptor proteins such as BLNK and SLP-76, which function as scaffolds that recruit both Tec kinases and PLCγ to form the osteoclastogenic signaling complex. This complex is crucial for efficient activation of calcium signaling required for the induction and activation of NFATc1, the key transcription factor for osteoclast differentiation.

(Tsukada et al., 1993). Targeted disruption of *Btk* alone did not result in an obvious bone phenotype in mice, and B cell immunoglobulin production was also not severely affected in this strain (Kerner et al., 1995). Therefore, it is possible that the mouse and human utilization of Tec family kinases is not strictly the same. Because immunoglobulin production is completely abrogated in the combined deficiency of Btk and Tec (Ellmeier et al., 2000), $Tec^{-/-}Btk^{-/-}$ mice may serve as a better model of XLA. Currently there is no report on abnormalities of bone metabolism in the XLA patients, but it will be of great significance to analyze bone density and quality in patients with primary immunodeficiencies in the future. These studies, together with others, including recent data on hyper-IgM syndrome (Lopez-Granados et al., 2007), will surely shed light on unexpected aspects of the linkage between the immune and bone systems.

Upstream and Downstream of Tec Kinases in the Osteoclastogenic Signal Transduction

Although phosphorylation of Tec kinases is dependent on Src family kinases in immune cells (Schmidt et al., 2004), c-Src deficiency or inhibition of Src family kinases by PP2 has little effect on osteoclast differentiation (T.K. and H.T., unpublished data). Although it is possible that other Src family members may compensate, to date there has been no clear evidence demonstrating an essential role for Src kinases in osteoclast differentiation; therefore, the kinases that phosphorylate the Tec kinases in osteoclasts remain to be elucidated.

Based on the in vitro data (Figure 4B), the phosphorylation of PLCγ by RANKL is mostly dependent on Btk and Tec. However, osteopetrosis in $Tec^{-/-}Btk^{-/-}$ mice is less severe than that in $DAP12^{-/-}FcR\gamma^{-/-}$ mice, and pathological bone loss is not completely abrogated in the $Tec^{-/-}Btk^{-/-}$ mice or the Tec kinase inhibitor-treated mice. It is conceivable that the loss of Btk and Tec is partly compensated by other Tec kinases or that an alternative kinase(s) partially functions as a PLCγ kinase during osteoclastogenesis.

Despite the crucial role of BLNK and SLP-76 in osteoclast differentiation in vitro, bone mineral density was not markedly increased in $Blnk^{-/-}Lcp2^{-/-}$ mice (M.S., T.K., and H.T., unpublished data). One explanation for this discrepancy is that BLNK and SLP-76 do play a substantially important role, but another adaptor molecule, such as cytokine-dependent hematopoietic cell linker (Clnk), may compensate for the loss in vivo. Although further studies are necessary to elucidate the mechanism(s), it is likely that membrane-bound or soluble factors, which induce or activate Clnk, are compensatorily upregulated only in vivo. In addition, as $Blnk^{-/-}Lcp2^{-/-}$ mice develop acute leukemia at a very high frequency (more than 90%; D.K., unpublished data), the onset of acute leukemia may affect bone homeostasis by producing soluble factors that activate osteoclastogenesis or inhibit osteoblastic bone formation.

Tec Family Kinases as Therapeutic Targets for Bone Diseases

$Tec^{-/-}Btk^{-/-}$ mice are resistant to OVX-induced bone loss, but $DAP12^{-/-}FcR\gamma^{-/-}$ mice, which exhibit more severe osteopetrosis, do lose bone after OVX in certain bones (Wu et al., 2007). These results suggest that osteoclastogenesis under pathological conditions is dependent on a signaling mechanism distinct from that in physiological bone remodeling. Whatever the detailed mechanism, the results indicate that the Tec kinases offer some auspicious therapeutic targets in the treatment of metabolic and inflammatory bone diseases (see Figure 6).

Considering the severe immunodeficiency in XLA, careful attention would obviously have to be given to side effects on other cell types, including B cells, if Tec kinases were systemically inhibited in order to treat metabolic bone diseases. In the case of inflammatory bone diseases such as rheumatoid arthritis, certain immunosuppressants have already been successfully utilized in the clinic, so the inhibition of these kinases may prove to be a potentially effective strategy for preventing bone destruction associated with inflammation. Undoubtedly, the suppression of molecules shared by immune and bone cells will require a very careful evaluation in both systems prior to any clinical application, but these efforts will be rewarded by the provision of a molecular basis for novel drug design in the future.

EXPERIMENTAL PROCEDURES

Mice and Analysis of Bone Phenotype

We previously described the generation of $Tec^{-/-}Btk^{-/-}$ (Ellmeier et al., 2000) and $DAP12^{-/-}FcR\gamma^{-/-}$ (Koga et al., 2004) mice. $Blnk^{-/-}$ (Hayashi et al., 2003) and $Lcp2^{-/-}$ (Pivniouk et al., 1998) mice were described previously. Histomorphometric and microradiographic examinations were performed as described (Koga et al., 2004).

In Vitro Osteoclast Formation, Ca^{2+} Measurement, and GeneChip Analysis

Bone marrow cells were cultured with 10 ng/ml M-CSF (R & D Systems) for 2 days, and they were used as BMMs. BMMs were cultured with 50 ng/ml RANKL (Peprotech) and 10 ng/ml M-CSF for 3 days. RANKL and M-CSF were added at these concentrations unless otherwise indicated. In the coculture system, bone marrow cells were cultured with calvarial osteoblasts with 10^{-8} M 1,25-dihydroxyvitamin D_3 and 10^{-6} M prostaglandin E_2. TRAP-positive MNCs (TRAP$^+$ MNCs, more than three nuclei) were counted. Proliferation rate was determined 24 hr after RANKL stimulation using Cell Proliferation ELISA Kit (Roche). Apoptosis was assayed 24 hr after RANKL stimulation using In Situ Cell Death Detection Kit (Roche). In Figure 2D, LFM-A13 (Calbiochem) was added at the same time as RANKL. Concentration of intracellular calcium was measured and GeneChip analysis was performed as described (Takayanagi et al., 2002).

Retroviral Gene Transfer

Retroviral vectors, pMX-Tec-IRES-GFP, pMX-Btk-IRES-GFP, pMX-Btk (R28C)-IRES-GFP, and pMX-Btk (R525Q)-IRES-GFP, were constructed by inserting cDNA fragments of Tec, Btk, Btk (R28C), or Btk (R525Q) (Takata and Kurosaki, 1996) into pMX-IRES-EGFP. Retrovirus packaging was performed by transfecting Plat-E cells with the plasmids as described previously (Morita et al., 2000). After 6 hr inoculation, BMMs were stimulated with RANKL for 3 days.

Depletion of CD19$^+$ B Cells

Bone marrow cells contain CD19$^+$ cells at the ratio of about 30% in WT mice and about 15% in *Tec*$^{-/-}$*Btk*$^{-/-}$ mice. CD19$^+$ cells were depleted with a magnetic sorter and anti-CD19 microbeads (MACS; Miltenyi Biotec). The purity was confirmed by FACS, and the population of CD19$^+$ B cells was less than 5% in these preparations.

Immunoblot Analysis, Immunofluorescence Staining, and Flow Cytometry

After being stimulated with RANKL and M-CSF, BMMs were harvested and cell lysates were subjected to immunoblot or immunoprecipitation analyses with specific antibodies against Tec (Mano et al., 1995), Btk, NFATc1, PLCγ1, BLNK, DAP12, β-actin (Santa Cruz), phospho-PLCγ2, PLCγ2, phospho-ERK, ERK, phospho-p38, p38, phospho-JNK, JNK, phospho-Akt, Akt, phospho-IKKα/β, IKKα, IKKβ (Cell Signaling), phospho-PLCγ1 (Biosource International), Itk, 4G10 (Upstate), and phospho-Btk (BD Biosciences). For immunofluorescence staining, cells were fixed with 4% paraformaldehyde, permeabilized, and then treated with the indicated specific antibodies followed by staining with Alexa Fluor 488- or 546-labeled secondary antibody (Molecular Probes). For flow cytometry, bone marrow cells were incubated with the anti-CD11b antibody (BD Biosciences) or control rat IgG for 30 min followed by staining with PE-conjugated anti-rat IgG antibody.

Ovariectomy-Induced Bone Loss

Seven-week-old female mice were ovariectomized under anesthesia. Three or 8 weeks after surgery, all of the mice were sacrificed and subjected to histomorphometric and microradiographic examinations. Parameters for trabecular bone (thickness, separation, and number) were calculated on the basis of data obtained from microcomputed tomography analysis as described (Aoki et al., 2006).

LPS-Induced Bone Destruction

Seven-week-old female mice were administered with a local calvarial injection of LPS (Sigma) at 25 mg/kg body weight with a simultaneous injection of LFM-A13 (20 mg/kg body weight) or saline and were analyzed after 5 days as described (Takayanagi et al., 2000). For the detection of IKK phosphorylation, the calvarial tissues were homogenized 15 min after LPS injection, and lysates were subjected to immunoblot analysis. The serum levels of TNF-α and IL-6 (30 min after LPS injection) were measured by ELISA kits (R & D Systems).

RANKL-Induced Bone Loss

Seven-week-old C57BL/6 female mice were intraperitoneally injected with 20 μg of GST or GST-RANKL (Oriental Yeast Co., Ltd.) three times at intervals of 24 hr. LFM-A13 (20 mg/kg body weight) or saline was injected 1 hr prior to GST-RANKL treatment. One and a half hours after the final injection, all of the mice were sacrificed and subjected to histomorphometric and microradiographic examinations. The serum level of Ca^{2+} was measured by Calcium C (Wako).

Statistical Analysis

All data are expressed as the mean ± SEM (n = 5). Statistical analysis was performed by using Student's t test or ANOVA followed by Bonferroni test when applicable (*$p < 0.05$; **$p < 0.01$; ***$p < 0.005$; n.s., not significant). Results are representative examples of more than four independent experiments. In Figure 6, statistical analysis was performed between WT and *Tec*$^{-/-}$*Btk*$^{-/-}$ mice (n = 5 per group) on the fold increase of each parameter.

SUPPLEMENTAL DATA

Supplemental Data include six figures and can be found with this article online at http://www.cell.com/cgi/content/full/132/5/794/DC1/.

ACKNOWLEDGMENTS

We thank T. Kitamura, H. Mano, K. Mori, Y. Tomimori, H. Yanagawa, and E. Miyamoto for reagents and technical advice. We also thank M. Isobe-Ohba, T. Nakashima, M. Asagiri, K. Nishikawa, H.J. Gober, K. Kuroda, S. Ochi, Y. Suzuki, and H. Murayama for helpful discussion and assistance. This work was supported in part by a Grant-in-Aid for Creative Scientific Research from the Japan Society for the Promotion of Science (JSPS); grants for the Genome Network Project from the Ministry of Education, Culture, Sports, Science, and Technology of Japan (MEXT); Health Sciences Research grants from the Ministry of Health, Labor, and Welfare of Japan; the Austrian Science Fund and the START Program of the Austrian Ministry of Education, Science, and Culture; and grants from Kanae Foundation for Life and Socio-Medical Science, Tokyo Biochemical Research Foundation, Yokoyama Foundation for Clinical Pharmacology, and Hayashi Memorial Foundation for Female Natural Scientists. No authors have any financial interest related to this work.

Received: June 12, 2007
Revised: November 8, 2007
Accepted: December 27, 2007
Published: March 6, 2008

REFERENCES

Aoki, K., Saito, H., Itzstein, C., Ishiguro, M., Shibata, T., Blanque, R., Mian, A.H., Takahashi, M., Suzuki, Y., Yoshimatsu, M., et al. (2006). A TNF receptor loop peptide mimic blocks RANK ligand-induced signaling, bone resorption, and bone loss. J. Clin. Invest. *116*, 1525–1534.

Asagiri, M., and Takayanagi, H. (2007). The molecular understanding of osteoclast differentiation. Bone *40*, 251–264.

Cherukuri, A., Dykstra, M., and Pierce, S.K. (2001). Floating the raft hypothesis: lipid rafts play a role in immune cell activation. Immunity *14*, 657–660.

Ellmeier, W., Jung, S., Sunshine, M.J., Hatam, F., Xu, Y., Baltimore, D., Mano, H., and Littman, D.R. (2000). Severe B cell deficiency in mice lacking the tec kinase family members Tec and Btk. J. Exp. Med. *192*, 1611–1624.

Faccio, R., Zou, W., Colaianni, G., Teitelbaum, S.L., and Ross, F.P. (2003). High dose M-CSF partially rescues the Dap12−/− osteoclast phenotype. J. Cell. Biochem. *90*, 871–883.

Fernandes, M.J., Lachance, G., Pare, G., Rollet-Labelle, E., and Naccache, P.H. (2005). Signaling through CD16b in human neutrophils involves the Tec family of tyrosine kinases. J. Leukoc. Biol. *78*, 524–532.

Grimbacher, B., Holland, S.M., Gallin, J.I., Greenberg, F., Hill, S.C., Malech, H.L., Miller, J.A., O'Connell, A.C., and Puck, J.M. (1999). Hyper-IgE syndrome with recurrent infections—an autosomal dominant multisystem disorder. N. Engl. J. Med. *340*, 692–702.

Ha, H., Kwak, H.B., Lee, S.K., Na, D.S., Rudd, C.E., Lee, Z.H., and Kim, H.H. (2003). Membrane rafts play a crucial role in receptor activator of nuclear factor κB signaling and osteoclast function. J. Biol. Chem. *278*, 18573–18580.

Hashimoto, S., Iwamatsu, A., Ishiai, M., Okawa, K., Yamadori, T., Matsushita, M., Baba, Y., Kishimoto, T., Kurosaki, T., and Tsukada, S. (1999). Identification of the SH2 domain binding protein of Bruton's tyrosine kinase as BLNK—functional significance of Btk-SH2 domain in B-cell antigen receptor-coupled calcium signaling. Blood *94*, 2357–2364.

Hata, D., Kawakami, Y., Inagaki, N., Lantz, C.S., Kitamura, T., Khan, W.N., Maeda-Yamamoto, M., Miura, T., Han, W., Hartman, S.E., et al. (1998). Involvement of Bruton's tyrosine kinase in FcεRI-dependent mast cell degranulation and cytokine production. J. Exp. Med. *187*, 1235–1247.

Hayashi, K., Yamamoto, M., Nojima, T., Goitsuka, R., and Kitamura, D. (2003). Distinct signaling requirements for Dμ selection, IgH allelic exclusion, pre-B cell transition, and tumor suppression in B cell progenitors. Immunity *18*, 825–836.

Horton, J.E., Raisz, L.G., Simmons, H.A., Oppenheim, J.J., and Mergenhagen, S.E. (1972). Bone resorbing activity in supernatant fluid from cultured human peripheral blood leukocytes. Science *177*, 793–795.

Horwood, N.J., Mahon, T., McDaid, J.P., Campbell, J., Mano, H., Brennan, F.M., Webster, D., and Foxwell, B.M. (2003). Bruton's tyrosine kinase is required for lipopolysaccharide-induced tumor necrosis factor alpha production. J. Exp. Med. *197*, 1603–1611.

Ishiai, M., Kurosaki, M., Pappu, R., Okawa, K., Ronko, I., Fu, C., Shibata, M., Iwamatsu, A., Chan, A.C., and Kurosaki, T. (1999). BLNK required for coupling Syk to PLCγ2 and Rac1-JNK in B cells. Immunity *10*, 117–125.

Jumaa, H., Bossaller, L., Portugal, K., Storch, B., Lotz, M., Flemming, A., Schrappe, M., Postila, V., Riikonen, P., Pelkonen, J., et al. (2003). Deficiency of the adaptor SLP-65 in pre-B-cell acute lymphoblastic leukaemia. Nature *423*, 452–456.

Karsenty, G., and Wagner, E.F. (2002). Reaching a genetic and molecular understanding of skeletal development. Dev. Cell *2*, 389–406.

Kerner, J.D., Appleby, M.W., Mohr, R.N., Chien, S., Rawlings, D.J., Maliszewski, C.R., Witte, O.N., and Perlmutter, R.M. (1995). Impaired expansion of mouse B cell progenitors lacking Btk. Immunity *3*, 301–312.

Kirchner, S.G., Sivit, C.J., and Wright, P.F. (1985). Hyperimmunoglobulinemia E syndrome: association with osteoporosis and recurrent fractures. Radiology *156*, 362.

Koga, T., Inui, M., Inoue, K., Kim, S., Suematsu, A., Kobayashi, E., Iwata, T., Ohnishi, H., Matozaki, T., Kodama, T., et al. (2004). Costimulatory signals mediated by the ITAM motif cooperate with RANKL for bone homeostasis. Nature *428*, 758–763.

Lopez-Granados, E., Temmerman, S.T., Wu, L., Reynolds, J.C., Follmann, D., Liu, S., Nelson, D.L., Rauch, F., and Jain, A. (2007). Osteopenia in X-linked hyper-IgM syndrome reveals a regulatory role for CD40 ligand in osteoclastogenesis. Proc. Natl. Acad. Sci. USA *104*, 5056–5061.

Mahajan, S., Ghosh, S., Sudbeck, E.A., Zheng, Y., Downs, S., Hupke, M., and Uckun, F.M. (1999). Rational design and synthesis of a novel anti-leukemic agent targeting Bruton's tyrosine kinase (BTK), LFM-A13. J. Biol. Chem. *274*, 9587–9599.

Mangla, A., Khare, A., Vineeth, V., Panday, N.N., Mukhopadhyay, A., Ravindran, B., Bal, V., George, A., and Rath, S. (2004). Pleiotropic consequences of Bruton tyrosine kinase deficiency in myeloid lineages lead to poor inflammatory responses. Blood *104*, 1191–1197.

Mano, H., Yamashita, Y., Sato, K., Yazaki, Y., and Hirai, H. (1995). Tec protein-tyrosine kinase is involved in interleukin-3 signaling pathway. Blood *85*, 343–350.

Mao, D., Epple, H., Uthgenannt, B., Novack, D.V., and Faccio, R. (2006). PLCγ2 regulates osteoclastogenesis via its interaction with ITAM proteins and GAB2. J. Clin. Invest. *116*, 2869–2879.

Minegishi, Y., Saito, M., Tsuchiya, S., Tsuge, I., Takada, H., Hara, T., Kawamura, N., Ariga, T., Pasic, S., Stojkovic, O., et al. (2007). Dominant-negative mutations in the DNA-binding domain of STAT3 cause hyper-IgE syndrome. Nature *448*, 1058–1062.

Mocsai, A., Humphrey, M.B., Van Ziffle, J.A., Hu, Y., Burghardt, A., Spusta, S.C., Majumdar, S., Lanier, L.L., Lowell, C.A., and Nakamura, M.C. (2004). The immunomodulatory adapter proteins DAP12 and Fc receptor γ-chain (FcRγ) regulate development of functional osteoclasts through the Syk tyrosine kinase. Proc. Natl. Acad. Sci. USA *101*, 6158–6163.

Morita, S., Kojima, T., and Kitamura, T. (2000). Plat-E: an efficient and stable system for transient packaging of retroviruses. Gene Ther. *7*, 1063–1066.

Perez de Diego, R., Lopez-Granados, E., Pozo, M., Rodriguez, C., Sabina, P., Ferreira, A., Fontan, G., Garcia-Rodriguez, M.C., and Alemany, S. (2006). Bruton's tyrosine kinase is not essential for LPS-induced activation of human monocytes. J. Allergy Clin. Immunol. *117*, 1462–1469.

Pivniouk, V.I., and Geha, R.S. (2000). The role of SLP-76 and LAT in lymphocyte development. Curr. Opin. Immunol. *12*, 173–178.

Pivniouk, V., Tsitsikov, E., Swinton, P., Rathbun, G., Alt, F.W., and Geha, R.S. (1998). Impaired viability and profound block in thymocyte development in mice lacking the adaptor protein SLP-76. Cell *94*, 229–238.

Ross, F.P., and Teitelbaum, S.L. (2005). $\alpha_v\beta_3$ and macrophage colony-stimulating factor: partners in osteoclast biology. Immunol. Rev. *208*, 88–105.

Schaeffer, E.M., Debnath, J., Yap, G., McVicar, D., Liao, X.C., Littman, D.R., Sher, A., Varmus, H.E., Lenardo, M.J., and Schwartzberg, P.L. (1999). Requirement for Tec kinases Rlk and Itk in T cell receptor signaling and immunity. Science *284*, 638–641.

Schmidt, U., Boucheron, N., Unger, B., and Ellmeier, W. (2004). The role of Tec family kinases in myeloid cells. Int. Arch. Allergy Immunol. *134*, 65–78.

Soriano, P., Montgomery, C., Geske, R., and Bradley, A. (1991). Targeted disruption of the c-*src* proto-oncogene leads to osteopetrosis in mice. Cell *64*, 693–702.

Takata, M., and Kurosaki, T. (1996). A role for Bruton's tyrosine kinase in B cell antigen receptor-mediated activation of phospholipase C-γ2. J. Exp. Med. *184*, 31–40.

Takayanagi, H. (2007). Osteoimmunology: shared mechanisms and crosstalk between the immune and bone systems. Nat. Rev. Immunol. *7*, 292–304.

Takayanagi, H., Ogasawara, K., Hida, S., Chiba, T., Murata, S., Sato, K., Takaoka, A., Yokochi, T., Oda, H., Tanaka, K., et al. (2000). T-cell-mediated regulation of osteoclastogenesis by signalling cross-talk between RANKL and IFN-γ. Nature *408*, 600–605.

Takayanagi, H., Kim, S., Koga, T., Nishina, H., Isshiki, M., Yoshida, H., Saiura, A., Isobe, M., Yokochi, T., Inoue, J., et al. (2002). Induction and activation of the transcription factor NFATc1 (NFAT2) integrate RANKL signaling in terminal differentiation of osteoclasts. Dev. Cell *3*, 889–901.

Teitelbaum, S.L., and Ross, F.P. (2003). Genetic regulation of osteoclast development and function. Nat. Rev. Genet. *4*, 638–649.

Theill, L.E., Boyle, W.J., and Penninger, J.M. (2002). RANK-L and RANK: T cells, bone loss, and mammalian evolution. Annu. Rev. Immunol. *20*, 795–823.

Tsukada, S., Saffran, D.C., Rawlings, D.J., Parolini, O., Allen, R.C., Klisak, I., Sparkes, R.S., Kubagawa, H., Mohandas, T., Quan, S., et al. (1993). Deficient expression of a B cell cytoplasmic tyrosine kinase in human X-linked agammaglobulinemia. Cell *72*, 279–290.

Walsh, M.C., Kim, N., Kadono, Y., Rho, J., Lee, S.Y., Lorenzo, J., and Choi, Y. (2006). Osteoimmunology: interplay between the immune system and bone metabolism. Annu. Rev. Immunol. *24*, 33–63.

Wong, B.R., Besser, D., Kim, N., Arron, J.R., Vologodskaia, M., Hanafusa, H., and Choi, Y. (1999). TRANCE, a TNF family member, activates Akt/PKB through a signaling complex involving TRAF6 and c-Src. Mol. Cell *4*, 1041–1049.

Wu, Y., Torchia, J., Yao, W., Lane, N.E., Lanier, L.L., Nakamura, M.C., and Humphrey, M.B. (2007). Bone microenvironment specific roles of ITAM adapter signaling during bone remodeling induced by acute estrogen-deficiency. PLoS ONE *2*, e586. 10.1371/journal.pone.0000586.

Int J Hematol (2008) 87:88–90
DOI 10.1007/s12185-007-0017-8

CASE REPORT

Successful treatment of chronic granulomatous disease with fludarabine-based reduced-intensity conditioning and unrelated bone marrow transplantation

Daiichiro Hasegawa · Masako Fukushima · Yuki Hosokawa · Hiroki Takeda · Keiichiro Kawasaki · Tomoyuki Mizukami · Hiroyuki Nunoi · Hiroshi Ochiai · Tomohiro Morio · Yoshiyuki Kosaka

Received: 25 May 2007 / Revised: 27 August 2007 / Accepted: 21 September 2007 / Published online: 7 December 2007

Abstract Allogeneic hematopoietic stem-cell transplantation (HSCT) for chronic granulomatous disease (CGD) with a reduced-intensity conditioning regimen can be expected to lead to less therapy-related mortality and late-onset impairment, whereas it has also been reported to increase the risk of unsustained mixed donor chimerism and late rejection after transplantation. Herein, we report a 4-year-old boy with CGD who was successfully treated with unrelated bone marrow transplantation with a reduced-intensity conditioning regimen (RIC). Fludarabine-based RIC, 4 Gy of total body irradiation, 120 mg/kg of cyclophosphamide, and 125 mg/m^2 of fludarabine, was adopted for transplantation, followed with 8.9×10^8/kg mononucleated donor cells infused without T-cell depletion. Although hematopoietic engraftment was rapidly obtained by day +17, he developed unstable donor chimerism. After tacrolimus withdrawal, the patient showed grade III acute graft-versus-host disease (GVHD), and subsequently reached full donor chimerism by day +61. Twelve months post-transplant, the patient has remained well with stable and durable engraftment, 100% donor chimerism, and normal superoxide production, without the requirement of donor lymphocyte infusions (DLI).

Keywords Chronic granulomatous disease · Unrelated bone marrow transplantation · Reduced intensity conditioning

D. Hasegawa (✉) · M. Fukushima · Y. Hosokawa · H. Takeda · K. Kawasaki · Y. Kosaka
Department of Hematology and Oncology, Kobe Children's Hospital, 1-1-1 Takakuradai, Suma, Kobe 654-0081, Japan
e-mail: hasegawa_kch@hp.pref.hyogo.jp

T. Mizukami · H. Nunoi
Department of Pediatrics, Miyazaki University School of Medicine, Miyazaki, Japan

H. Ochiai · T. Morio
Center for cell therapy, Tokyo Medical and Dental University, Tokyo, Japan

1 Introduction

Chronic granulomatous disease (CGD) is a primary immunodeficiency caused by impaired phagocyte killing of intracellular pathogens, characterized by recurrent, often life-threatening bacterial and fungal infections and by granuloma formation in vital organs. It results from mutation in any one of four subunits of a nicotinamide adenine dinucleotide phosphate oxidase of phagocytic cells ($gp91^{phox}$, $p47^{phox}$, $p67^{phox}$, and $p22^{phox}$) [1]. Although the prognosis of CGD has markedly improved due to prophylactic treatment for infections, including the induction of interferon-gamma therapy, annual mortality is still between 2 and 5% [2]. Allogeneic hematopoietic stem-cell transplantation (HSCT) is an alternative to conventional treatment for CGD, but a high transplantation-related mortality rate [3] and high risk of graft rejection have lowered its therapeutic efficacy [4]. We here in report a 4-year-old boy with CGD who was successfully treated with unrelated bone marrow transplantation with a fludarabine-based reduced-intensity conditioning regimen (RIC).

2 Case report

A 4-year-old boy with CGD was admitted to our hospital in August 2005. He had had recurrent bacterial and fungal infections from early infancy, and CGD was diagnosed by

reduced NADPH oxidase (0%), confirmed by $gp91^{phox}$ expression analysis when he was 1 year old. His elder brother was also diagnosed with CGD, and died of fungal pneumonia at the age of 10 years old. There was no HLA-identical HSCT donor in his family. He received anti-infectious prophylaxis consisting of itraconazole and sulfamethoxazole/trimethoprim. Diagnostic imaging at 3 years of age showed intraperitonial granulation tissue formation and hyperplasia of the intestinal tract, resulting from having intussusceptions two times. Interferon gamma therapy had been given for 6 months before transplantation, but subsequently failed. Thus, allogeneic bone marrow transplantation from an HLA-matched volunteer donor was planned.

At 4 years of age, he received allogeneic bone marrow transplantation from an HLA-matched unrelated donor in March 2006. Donor and recipient HLA matching was confirmed by serotyping and molecular typing of the HLA class I and II loci, respectively. We used a RIC for transplantation with total body irradiation at a dose of 2 Gy (days −8 and −7) without use of the gonadal shield, cyclophosphamide at a dose of 60 mg/kg (days −3 and −2) and fludarabine at a dose of 25 mg/m^2 (days −6, −5, −4, −3 and −2), because the patient had been chronically ill, showing intermittent fever and moderate elevation of CRP values, which was thought to be due to chronic enterocolitis. Repeated stool and blood cultures were negative for bacteria and fungi. Just before transplantation, laboratory findings included increased C-reactive protein (2.39 mg/dl) and a normal beta-D-glucan level. Latex agglutination test for serum *Aspergillus* and serum *Candida* antigens were negative.

A cell dose of 8.9×10^8/kg mononucleated cells was infused to the patient without T-cell depletion. GVHD prophylaxis consisted of tacrolimus (0.03 mg/kg/day i.v. continuous infusion from day −1) and short-term methotrexate (10 mg/m^2 i.v. on day +1, 7.5 mg/m^2 i.v. on days +3 and +6). He was also nursed in a high-efficiency, particulate-air-filtered protected environment, and underwent oral gut decontamination. He received *Peumocystis carinii* prophylaxis by sulfamethoxazole/trimethoprim, which was interrupted after transplantation until neutrophil recovery confirmed. Post-transplant regimen also included acyclovir, ursodeoxycholic acid and intravenous immunoglobulin therapy. Chimerism was studied via the analysis of informative microsatellite DNA sequences. The oxidase-positive neutrophils were detected by flow cytometry with the use of a dihydrorhodamine oxidation assay.

During the conditioning therapy for transplantation, prolonged fever rapidly resolved and C-reactive protein values also decreased to within normal ranges. A total of 300 μg/m^2 of granulocyte-colony stimulating factor was commenced on day +5 post-transplant. The patient engrafted rapidly. He achieved an absolute neutrophil count of 0.5×10^9/l by day +17. Chimerism analysis revealed 62.5% donor cell engraftment by day +21, and 39.3% donor cell engraftment additively decreased by day +34, respectively. To achieve complete chimerism, we stopped all immunosuppressants by day +39, because he had no GVHD confirmed at that time. Subsequently, grade III acute GVHD of his skin and gut were clinically confirmed on day +55, followed by full converted donor chimerism and normal superoxidase production by day +61. He was treated again with tacrolimus and 2 mg/kg of prednisolone for GVHD, and all GVHD symptoms disappeared by day +80. Reactivation of his Cytomegalovirus antigenemia was detected on day +65, and treated with ganciclovir with good response. Flow cytometric analysis with the use of a dihidrorhodamine

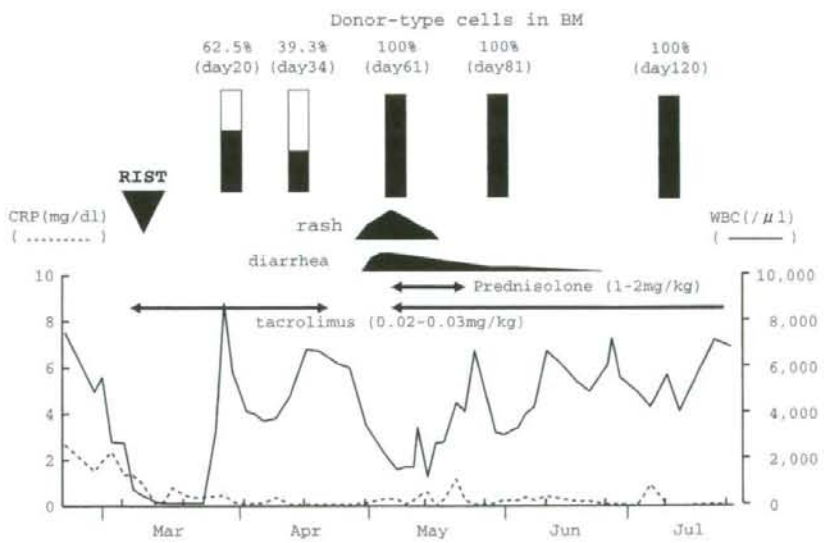

Fig. 1 Clinical course after unrelated bone marrow transplantation. RIST indicates reduced intensity stem cell transplantation. In the upper section of the figure, the donor-type cells in the bone marrow are represented as *black-lacquered*

oxidation assay showed that oxidase-positive neutrophils were detected as 100% of engrafted cells since then. Twelve months post-transplant, the patient has remained well, with stable and durable engraftment, 100% donor chimerism, normal superoxide production, without donor lymphocyte infusion (DLI) requirement (Fig. 1).

3 Discussion

Allogeneic HSCT is the curative therapy for CGD, especially in patients with no inflammatory or infectious lesions at transplant with an excellent disease-free survival rate (DFS). A survey of European Group for blood and marrow transplantation (EBMT) has advocated myeloablative regimens, mostly consisting of busulfan (16 mg/kg) and cyclophosphamide (200 mg/kg), and T-cell replete allografts from HLA-matched related donors, which provided excellent results in low-risk CGD patients (15 children and 1 adult) with no overt infectious complications at transplant and a DFS of 100% [3]. However, in the EBMT report, inadequately high rates of severe acute GVHD and pulmonary infectious complication with a transplant-related mortality of 36% (4 of 11 patients) were also observed in advanced CGD patients with active inflammation due to granulomatous colitis or active infectious disease. Thus, transplant-related mortality with standard myeloablative transplantation regimens, especially in advanced CGD, has been a major obstacle to the more widespread use of allogeneic HSCT.

Horwitz et al. recently reported promising results in the treatment of 10 advanced CGD patients with the combination of a nonmyeloablative regimen consisting of cyclophosphamide, fludarabine, and antithymocyte globulin and the use of a T-cell depleted HLA-identical allograft [5]. This US trial demonstrated that seven out of 10 patients were successfully cured of the disease, even though two patients rejected their graft and DLI led to GVHD in three patients, which was fatal in one case. There are also several reports of successful outcomes for CDG with fludarabine-based RIC [6–9], while most of them consisted of transplant from HLA-matched related donors. Furthermore, T-cell depletion could be a promising approach to reduce the incidence of GVHD, while it could be associated with an increased risk of infectious complications and graft rejection. Thus, RIC is associated with a lower toxity from the conditioning agents and may be an alternative option for CGD, while it still carries a significant risk of graft rejection and GVHD, particularly if DLI have to be used to ensure engraftment.

A national survey of HSCT for CGD in Japan has shown fairly high survival rate (22 of 28), in which the survival rate of HSCT from HLA-matched siblings were comparable to that of HSCT from HLA-matched unrelated donors, whereas that of cord blood transplantation were improperly poor (2 of 4) [10]. Recently, nonmyeloablative conditioning regimens, mostly consisting cyclophosphamide and fludarabine, have been preferred, while the myeloablative conditioning, consisted of busulfan and cyclophosphamide, have been initially performed. However, inadequately high rates of development of unsustained mixed chimerism with the requirement of DLIs were also demonstrated in the patients with RIC by cyclophosphamide and fludarabine. In current case, we adapted fludarabine-based RIC without T-cell deletion for transplantation, because it is not allowed to manipulate unrelated donor allografts for DLIs, and also increased the total body irradiation dose to 4 Gy to ensure engraftment. Taken together, although standard regimens for transplantation of advanced CGD have not been established, our present case encourages the consideration of unrelated HSCT with fludarabine-based RIC for patients with CGD, even if they have infectious complications and no suitable related donors.

References

1. Lekstrom-Himes JA, Gallin JI. Advances in immunology: immunodeficiency diseases caused by defects in phagocytes. N Engl J Med. 2000;343:1703–4.
2. Winkelstein JA, Marino MC, Johnston RB Jr, et al. Chronic granulomatous disease. Report on a national registry of 368 patients. Medicine. 2000;79(3):155–9.
3. Seger RA, Gungor T, Belohradsky BH, et al. Treatment of chronic granulomatous disease with myeloablative conditioning and an unmodified hemopoietic allograft: a survey of the European experience, 1985–2000. Blood. 2002;100(13):4344–50.
4. Nagler A, Ackerstein A, Kapelushnik J, Or R, Naparstek E, Slavin S. Donor lymphocyte infusion post-non-myeloablative allogeneic peripheral blood stem cell transplantation for chronic granulomatous disease. Bone Marrow Transplant. 1999;24(3):339–42.
5. Horwitz ME, Barrett AJ, Brown MR, et al. Treatment of chronic granulomatous disease with nonmyeloablative conditioning and a T-cell-depleted hematopoietic allograft. N Engl J Med. 2001;344(12):881–8.
6. Nicholson JAT, Wynn RF, Carr TF, Will AM, et al. Sequential reduced- and full-intensity allografting using same donor in a child with chronic granulomatous disease and coexistent, significant comorbidity. Bone Marrow Transplant. 2004;34(11):1009–10.
7. Gungor T, Halter J, Klink A, Junge S. Successful low toxicity hematopoietic stem cell transplantation for high-risk adult chronic granulomatous disease patients. Transplantation. 2005;79(11):1596–606.
8. Sastry J, Kakakios A, Tugwell H, Shaw PJ. Allogeneic bone marrow transplantation with reduced intensity conditioning for chronic granulomatous disease complicated by invasive Aspergillus infection. Pediatr Blood Cancer. 2006;47(3):327–9.
9. Kikuta A, Ito M, Mochizuki K, et al. Nonmyeloablative stem cell transplantation for nonmalignant diseases in children with severe organ dysfunction. Bone Marrow Transplant. 2006; 38(10):665–9.
10. Nunoi H. Two breakthroughs in CGD studies. Nihon Rinsho Meneki Gakkai Kaishi. 2007;30(1):1–10.

ミニ特集

ここまで分かっている免疫不全症候群

9．Ataxia telangiectasia の臨床的特徴

—全国調査から明らかになったこと—

東京医科歯科大学大学院発生発達病態学分野　森尾友宏（もりおともひろ）

KEY WORDS
ataxia telangiectasia
ATM
diagnosis
cerebellar ataxia
immunodeficiency

Tomohiro Morio

はじめに

Ataxia telangiectasia（以後 AT と省略）は「毛細血管拡張性小脳失調症」と訳されている，頻度は高くないが，幼児期からの小脳失調症で鑑別すべき重要な疾患である。毛細血管拡張症は遅れて出現するが，進行性の小脳失調症に加えて，高頻度の悪性腫瘍発生，免疫不全症が臨床上大きな問題になる[1)2)]。

発症頻度は欧米では40,000～100,000人に1人とされている。したがって保因者は100人から160人に1人程度であると推測される。責任遺伝子は11番染色体上の ATM（Ataxia telangiectasia mutated）であり，常染色体劣性の遺伝形式をとる。

Ⅰ．病態生理[1)3)]

ATM は DNA 損傷修復反応（DNA damage response：DDR），特に二重鎖 DNA（double strand DNA：dsDNA）切断修復に重要な役割を果たす分子であり，生体にとって危害の大きい dsDNA 切断に際して活性化し，下流の様々な鍵となる分子をリン酸化することにより，細胞周期を制御し，DNA 切断修復あるいはアポトーシスに関与する。dsDNA 切断は，Mre11/Rad50/NBS 1（MRN 複合体）によって感知され，ATM を損傷の場に誘導する。ATM は MRN 複合体をリン酸化するとともに，Chk 2，SMC 1，p53などの分子をリン酸化して，ダ

〒113-8519　東京都文京区湯島1-5-45

メージの加わった細胞周期や，刺激の種類に応じて，さらに細胞周期停止，非相同 DNA 末端結合，相同組換え，細胞死などを誘導する。

DNA 損傷は電離放射線，紫外線，薬剤などの外的要因のみならず，日々の細胞代謝（活性酸素産生，複製停止など）において観察される事象である。1つの細胞において1日に10,000のプリン残基が欠失しているとされている。dsDNA 切断はその回数はさらに少ないが，細胞分裂や，遺伝子再構成・体細胞突然変異など免疫学的多様性を生み出す機構において必須で，そのたびに DDR が起きていることになる。

このように ATM は，DNA 損傷を受ける場において発動・活性化し，腫瘍化のバリアとして働いているので，その欠損は高頻度悪性腫瘍発生という表現型として観察される。また V（D）J 再構成，免疫グロブリンクラススイッチ（Immunoglobulin class switch recombination：IgCSR）においても，ATM がシナプス形成や切断修復に関与するために，リンパ球発生や CSR に関与する。一方，ATM は免疫グロブリン体細胞突然変異（Immunoglobulin somatic hypermutation：SHM）には不可欠でないことが示されている[4]。

一番大きな問題である小脳失調に関しては，Purkinje 細胞の異常が認められるものの，なぜ小脳に比較的特異的に症状が出現するのかは未だに大きな謎である。ATM 欠損マウスで明らかな小脳失調が現れないことも研究の進展を阻んでいるといえる。

II. 日本での AT 患者全国調査

日本での AT 患者の実態が明らかでなかったために，2005年9月に厚生労働省難治性疾患克服研究事業「原発性免疫不全症候群に関する調査研究」班の活動のなかで，初めての全国調査を行った。全国665の病院の神経内科，小児科，血液腫瘍科，リハビリ科などを中心とする1,223部局にアンケートを送付したところ，92名の AT の可能性のある患者について一次情報が集まった。さらに二次アンケートを行い，より詳細な情報を収集したところ（**表1**），重複患者，AT ではない方を除外して合計89名の AT 患者が登録された。そのうち10名では，説明と同意の元に，ATM タンパク質発現解析および遺伝子変異解析を行った。

神経内科医，小児科医フォローアップの比率はほぼ半々であるが，小児科では神経専門医による診療が多く，初発症状からも理解できる。悪性腫瘍の発生，感染症の反復をもって血液・腫瘍・免疫専門医と併診になることが多いようである。

表1　二次アンケート内容

基本情報
- 生年月，性別
- 家族歴（悪性腫瘍）
- 診断年月日，経過および死亡原因

臨床症状
- 小脳失調（体幹失調，構語障害，流涎，眼球運動の失行あるいは眼振，車いすの使用，舞踏病，振戦）と発症時期
- 毛細血管拡張，部位と発症時期
- 感染症の種類と発症時期
- 悪性腫瘍の種類・表現型・遺伝子異常・治療の有害事象，治療結果
- 自己免疫疾患・内分泌疾患（糖尿病，甲状腺機能，そのほか）
- そのほかの特記すべき症状

検査所見
- 遺伝子変異
- 染色体異常とその種類
- 免疫学的所見：リンパ球サブセット・TCR レパートア，免疫グロブリン値・EBV 抗体価
- 検査データ（α-fetoprotein，CEA）
- 脂質・代謝関連所見およびデータ
- 知能テスト・画像所見

治療内容

III. AT 患者全国調査から明らかになった臨床症状

1. 発症年齢，診断年齢（疾患名にとらわれると診断が遅れる）

小脳失調が明らかになった年齢の中央値（範囲）は18カ月（8カ月～5歳6カ月）であり，毛細血管拡張は6歳8カ月（1歳8カ月～13歳6カ月）に観察されている。診断は6歳9カ月（11カ月～24歳6カ月）時になされているが，おそらくは毛細血管拡張とあわせて臨床診断となっているものと思われる。これらの年齢は Cabana MD らの報告[5]と大きな差はない。

注意すべきは毛細血管拡張は半数が6歳以上となってから明らかになることであり，Ataxia telangiectasia という疾患名にとらわれると診断時期が遅くなり，X線撮影や悪性腫瘍に対する化学療法などに際して払うべき注意が行えなくなる可能性がある。2歳以降の小脳失調症で α fetoprotein が高値であれば，AT を積極的に疑う必要がある（表2の診断の手引きを参照）。

生存者の年齢の中央値（範囲）は14歳5カ月（4歳～28歳7カ月），逝去者では19歳0カ月（5歳9カ月～31歳10カ月）であった。また生存年齢中央値は26.0歳である。

2. 神経症状（図1）

まとめを図1に示す。全員で体幹失調を認め，注意深い観察あるいは補助器具を用いれば眼球失行（apraxia）も明らかである。舞踏病も3割程度で認められ注意を要する。

表2　AT の診断基準（AT Children's ProJect HP）
（http://www.communityatcp.org/NETCOMMUNITY/Page.aspx?pid=590&srcid=588より改変）

［症状］
1. 歩行開始と共に明らかになる歩行失調（体幹失調）：必発症状
   徐々に確実に進行（2歳から5歳までの間には進行がマスクされることもある）．
2. 小脳性構語障害・流涎
3. 眼球運動の失行，眼振
4. 舞踏病アテトーゼ（全例ではない）
5. 低緊張性顔貌
6. 眼球結膜・皮膚の毛細血管拡張
   ←6歳までに50%，8歳時で90%が明らかに．
7. 免疫不全症状（反復性気道感染症）
   ←30%では免疫不全症状を認めない．
8. 悪性腫瘍：発生頻度が高い．
9. そのほか（認めることがあるもの）：
   発育不良
   内分泌異常（耐糖能異常：インスリン非依存性糖尿病），
   皮膚，頭髪，血管の早老性変化

［検査データ］
1. α フェトプロテインの上昇（2歳以降：95%以上で）
2. CEA の増加（認めることがある）
3. IgG（IgG 2），IgA，（IgE）の低下（70%で）
4. CD 4 細胞中CD4＋CD45RA＋細胞の比率の低下
5. そのほか：
   電離放射線高感受性
   リンパ球，線維芽細胞の染色体異常

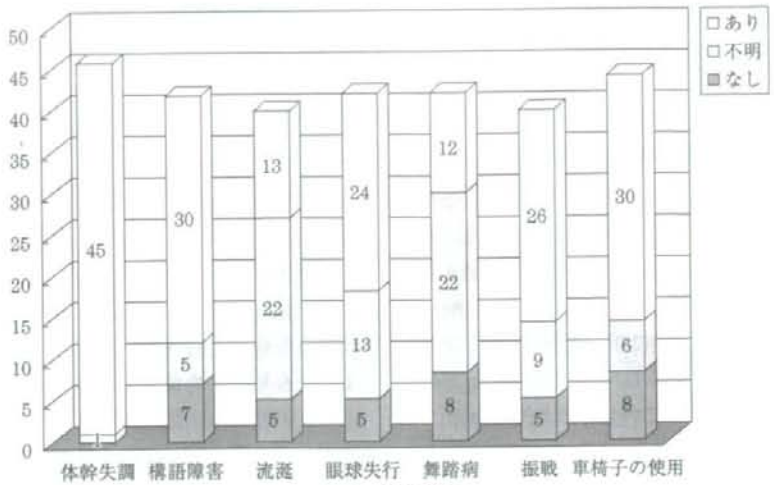

図1　神経症状

誤嚥性肺炎などから嚥下障害の評価は重要であり，Johns Hopkins 大学の AT センターでは嚥下無呼吸（deglutition apnea）の持続と嚥下前後の呼気流量を測定することにより管理に役立てているようである。

3．悪性腫瘍

悪性腫瘍は76名中17例に発症し，12症例で詳細な情報が得られた。6例は急性リンパ性白血病（T：4例，PreB：2例），4例は悪性リンパ腫，1例が組織球症，1例は胆管癌である。このうち発症後1年の時点で寛解に入っていたのは T-ALL の2症例と，悪性リンパ腫の1例のみである。予想されることではあるが，化学療法薬に対する有害事象も目立ち，急激な多臓器不全，心不全，遅発性出血性膀胱炎などを認めている点に注意を要する。特に，PreB-ALL の発症は AT の診断前であることも経験する。

4．感染症

AT では日和見感染症が稀とされている[6]。実際に感染症は神経症状が進んでからの誤嚥性肺炎など細菌感染症が前面に立っている。AT ではT細胞減少症を認めることが多く，検査データからは予想に反する結果といえる。今回の解析からは，AT では持続性 EBV 感染症，難治性 VZV 感染症，ヘルペス脳炎などヘルペス属感染症が重症化することが明らかになった。また長期入院を要する麻疹肺炎も2症例で認められている。CMV 感染症，カリニ肺炎，真菌感染症は稀だが，早期からの細菌感染症などにマスクされているだけの可能性もあり注意が必要と考えられる。

5．免疫異常

AT では CD3＋，CD4＋，CD8＋，CD20＋細胞の減少はそれぞれ66%，76%，39%，78%で認められた。CD4＋CD45RA＋細胞の減少も特徴的である。T細胞減少を反映して TREC（T cell receptor excision circle）は全例で低下していた（既報と一致する[7]）。T細胞減少はまた，上記の重症ウイルス感染症と相関が認められた。

免疫グロブリンでは16%で IgG＜500mg/dℓ，34%で IgA＜50mg/dℓであった。低 IgG 血症のうち，3例は panhypogammaglobulinemia であり，5例は HyperIgM の表現型をとっていた。これらの患者では CD27陽性メモリーB細胞数が低下していた。免疫異常は進行性ではないことが示されている[6]。

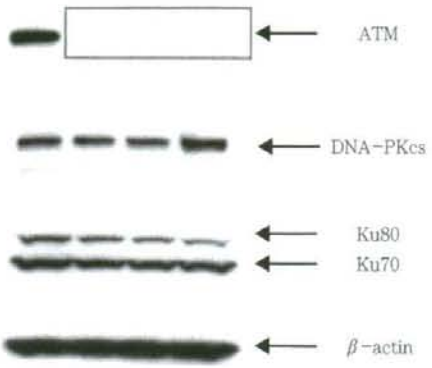

図2　ATの診断（anti-ATM immunoblot）
第一レーンは正常コントロール，第二から四レーンはAT患者サンプル．

6．診断（図2）

ATMは66のexonからなる長大な遺伝子であり，また患者での変異はintron領域にも多いため，その塩基配列決定には大きな労力を要していたが，現在はPIJDを通じてATMの遺伝子解析が可能である。しかし診断のうえで欠かせないのが，Westernblot法によるATMタンパクの確認であり，当施設ではT細胞を*in vitro*で増殖させるか，あるいはEBV-LCLを作成して実施している。この際にはATR，Mre11，Rad50，NBS1，Ku70/80，DNA-PKcsも解析し，漏れのないようにしている。

最近教室の高木らは，電離放射線照射あるいはH_2O_2刺激後のATMリン酸化をFA-CSで測定する系を立ち上げた（Leukemia，in press）。この方法は簡便で半日以内に結果が出るのみならず，hetero異常も検出可能である。スクリーニングとしては最適の方法と考えている。

7．死亡原因

死因の第一位は感染症である。今回のアンケートでは感染症で死亡した18名のうち5例が化学療法中になくなっている。そのほか，腫瘍死も3名と目立っている。何よりも誤嚥性肺炎対策が急務と考える。

おわりに

ATの臨床症状を中心に概説した。ATは神経医により気づかれるが，初期診断には難渋することがある。その点で，αFPを参考にしつつ，phospho-ATM FACSなどで第一次スクリーニングとすることが大切であろう。ATと判明したら，血液腫瘍医，内分泌専門医などとの連携が必須である。ATMについての基礎研究の進歩は目覚ましいが，小脳失調の発症原因解明など神経分野での検討が立ち遅れている。今後この領域に神経医が参画することを期待したい。

特に治療の開発が遅れている。酸化防止薬としてのN-acetyl cysteineや，exon skippingをブロックするantisence morpholinoによる治療，readthroughを狙った治療などが試みられているが，実用には不十分である。

私どもの施設は日本のAT診断センターに指定されていて，診断や治療について相談に応じている。神経症状の評価については，都立神経病院神経小児科 熊田聡子医師が国際ワークショップでトレーニングを受けてきている。何かの際にはご連絡いただければ幸いである。また実際のフォローに際しては，AT Children's Project HP（http://www.atcp.org/）に詳しい情報が掲載されており，ぜひ参照していただきたい。

文　献

1) Gatti RA, Becker-Catania S, Chun HH et al：The pathogenesis of ataxia-telangiectasia. Learning from a Rosetta Stone. Clin Rev Allergy Immunol 20：87～108, 2001
2) Perlman S, Becker-Catania S, Gatti RA：Ataxia-telangiectasia：diagnosis and treatment. Semin Pediatr Neurol 10：173～182, 2003
3) Shiloh Y：The ATM-mediated DNA-damage response：taking shape. Trends Biochem Sci

31 : 402～410, 2006
4) Pan-Hammarstrom Q, Dai S, Zhao Y et al : ATM is not required in somatic hypermutation of VH, but is involved in the introduction of mutations in the switch mu region. J Immunol 170 : 3707～3716, 2003
5) Cabana MD, Crawford TO, Winkelstein JA, Christensen JR, Lederman HM : Consequences of the delayed diagnosis of ataxia-telangiectasia. Pediatrics 102 : 98～100, 1998
6) Claret Teruel G, Giner Munoz MT, Plaza Martin AM, Martin Mateos MA, Piquer Gibert M, Sierra Martinez JI : Variability of immunodeficiency associated with ataxia telangiectasia and clinical evolution in 12 affected patients. Pediatr Allergy Immunol 16 : 615～618, 2005
7) Giovannetti A, Mazzetta F, Caprini E et al : Skewed T-cell receptor repertoire, decreased thymic output, and predominance of terminally differentiated T cells in ataxia telangiectasia. Blood 100 : 4082～4089, 2002

☆ ☆ ☆ ☆ ☆ ☆

European Journal of Haematology ISSN 0902-4441

ORIGINAL ARTICLE

$CD16^+$ $CD56^-$ NK cells in the peripheral blood of cord blood transplant recipients: a unique subset of NK cells possibly associated with graft-versus-leukemia effect

Xuzhang Lu[1], Yukio Kondo[1], Hiroyuki Takamatsu[1], Kinya Ohata[1], Hirohito Yamazaki[2], Akiyoshi Takami[3], Yoshiki Akatsuka[4], Shinji Nakao[1]

[1]Cellular Transplantation Biology, Kanazawa University Graduate School of Medical Science, Kanazawa, Ishikawa, Japan; [2]The Protected Environmental Unit, Kanazawa University Hospital, Kanazawa, Ishikawa, Japan; [3]Division of Transfusion Medicine, Kanazawa University Hospital, Kanazawa, Ishikawa, Japan; [4]Division of Immunology, Aichi Cancer Research Institute, Nagoya, Aichi, Japan

Abstract

A marked increase in $CD16^+$ $CD56^-$ NK cells in the peripheral blood (PB) was observed in a cord blood transplant (CBT) recipient with refractory acute myeloid leukaemia (AML) in association with attaining molecular remission. $CD16^+$ $CD56^-$ NK cells isolated from the patient became $CD16^+CD56^+NKG2D^+$ when they were cultured in the presence of IL-2. Although cultured $CD16^+CD56^-$ NK cells retained the killer-cell immunoglobulin receptor (KIR)-ligand (KIR-L) specificity and the patient's leukemic cells expressed corresponding KIR ligands, they killed patient's leukemic cells expressing ULBP2. The cytotoxicity by cultured $CD16^+CD56^-$ NK cells was abrogated by anti-ULBP2 antibodies. When leukemic cells obtained at relapse after CBT were examined, both the ULBP2 expression and susceptibility to the cultured NK cells decreased in comparison to leukemic cells obtained before CBT. An increase in the $CD16^+CD56^-$ NK cell count (0.5×10^9/L or more) in PB was observed in seven of 11 (64%) CBT recipients but in none of 13 bone marrow (BM) and eight peripheral blood stem cell (PBSC) transplant recipients examined during the similar period after transplantation. These findings suggest an increase in $CD16^+CD56^-$ NK cells to be a phenomenon unique to CBT recipients and that mature NK cells derived from this NK cell subset may contribute to the killing of leukemic cells expressing NKG2D ligands *in vivo*.

Key words $CD56^+CD16^-$ NK cell; NKG2D; graft-versus-leukemia; cord blood transplantation

Correspondence Shinji Nakao, Cellular Transplantation Biology, Kanazawa University Graduate School of Medical Science, Kanazawa University Hospital, 13-1 Takara-machi Kanazawa, Ishikawa 920-8640, Japan. Tel: +81-76-265-2274; Fax: +81-76-234-4252; e-mail: snakao@med3.m.kanazawa-u.ac.jp

Accepted for publication 6 March 2008

doi:10.1111/j.1600-0609.2008.01073.x

Cord blood transplantation (CBT) is being increasingly used for treatment of hematologic malignancies because its efficacy in the treatment of adult patients has been proven based on the findings of recent studies (1–4). One possible drawback of CBT is the less potent graft-versus-leukemia (GVL) effect than that of bone marrow transplantation (BMT) or peripheral blood stem cell transplantation (PBSCT) due to the immaturity of T cells contained in the cord blood (CB) graft (5). However, a recent study has shown the relapse rate after CBT to be comparable to that after BMT or PBSCT from human leukocyte antigen (HLA) matched sibling donors (1). Moreover, an analysis on the outcome of CBT for adult patients with acute myeloid leukaemia (AML) in Japan revealed that the rate of leukemic relapse after HLA-mismatched CBT was lower than that after HLA-matched CBT despite the fact that the incidence of graft-versus-host disease (GVHD) was similar between the two groups (Cord Blood Bank Network of Japan; unpublished observation). These clinical findings suggest that immunocompetent cells other than T cells may mediate the GVL effect after CBT.

Natural killer (NK) cells play a major role in the development of GVL effect after an HLA-mismatched stem cell transplantation (SCT) (6, 7). The GVL effect by NK cells depends on the presence of

HLA-mismatches and T cell recovery after SCT (8). Because CBT is often carried out from HLA-mismatched donors and is also associated with delayed T cell recovery (9–11), NK cells may be more likely to contribute to the development of GVL effect after CBT than after BMT or PBSCT. Few studies, however, have previously focused on the GVL effect by NK cells after CBT.

CB has a unique subset of NK cells characterized by a phenotype CD16$^+$CD56$^-$ (12–14). This NK cell subset is thought to be immature NK cells capable of differentiating into CD16$^+$CD56$^+$ NK cells (15). We recently observed an apparent increase in this NK cell subset in a patient who underwent reduced-intensity CBT for the treatment of relapsed AML after PBSCT from an HLA-compatible sibling donor. The patient achieved a molecular remission of AML in association with the NK cell increase. This observation prompted the characterization of CD16$^+$CD56$^-$ NK cells of this patient and other patients after allogeneic SCT. The present study revealed that CD16$^+$CD56$^-$ NK cells may potentially play a role in the development of the GVL effect in patients whose leukemic cells express NKG2D ligands.

Materials and methods

Patients

Peripheral blood (PB) was obtained from 11 CBT, 13 BMT (10 from related and three from unrelated donors), and eight PBSCT patients 2–135 months after transplantation. None of the patients had active graft-versus-host disease requiring corticosteroids at time of sampling or signs of infection. The original diseases of the CBT recipients included AML in four, non-Hodgkin's lymphoma (NHL) in four, myelodysplastic syndromes (MDS) in two and renal cell carcinoma in one. In the BMT recipients, those were AML in four, acute lymphoblastic leukemia (ALL) in four, MDS in three, chronic myeloid leukaemia (CML) in one, and aplastic anaemia (AA) in one while in the PBSCT recipients, those were AML in four, ALL in one, biphenotypic leukemia in two and NHL in one. All CBT recipients received an HLA-mismatched graft; the number of HLA mismatches between donor and recipient were two in seven, three in three and four in one. No HLA mismatch was observed between each donor and the BMT or PBSCT recipient except for six PBSCT recipients whose mismatches with their donors was one in two, two in one and three in one. This study was approved by our institutional review board and all patients gave their informed consent for the phenotypic and functional analyses of their peripheral blood mononuclear cells (PBMCs).

Phenotype analysis of PBMC after SCT and leukemia cells

The cell surface phenotype was determined by three-color flow cytometry. The cells were stained with various monoclonal antibodies (mAbs) specific to cell surface proteins including CD3, CD56, CD16, CD158a, CD158b (Becton Dickinson Pharmingen), NKG2A, NKG2D, NKp30, NKp44 and NKp46 (Beckman Coulter, Marseille, France). The expression of NKG2D ligands on leukemic cells from a CBT recipient was determined using mAbs specific to MICA/B (Becton Dickinson Pharmingen), ULBP1, ULBP2 and ULBP3 (R&D Systems, Minneapolis, MN).

Cell separation

PBMCs were isolated using density gradient centrifugation. NK cells were enriched by negative selection using immunomagnetic beads (Dynal NK cell isolation kit; Dynal Biotech, Lake success, NY) according to the manufacturer's recommendation (16). NK cell purity was confirmed by flow cytometry. CD16$^+$CD56$^+$ and CD16$^+$CD56$^-$ NK cells were separated from the enriched NK cells with anti-CD56-coated microBeads (MACS) by passing them through two sequential large-scale columns (Milteny Biotec, Gladbach, Germany) according to the manufacturer's instructions. CD158b$^+$ and CD158b$^-$ NK cells were separated with anti-CD158b-FITC Abs and anti-FITC microbeads.

NK cell culture

Isolated 2×10^6 CD16$^+$CD56$^+$ and CD16$^+$CD56$^-$ subsets were cultured with or without 2×10^5 irradiated (45 Gy) K562 cells transfected with the membrane-bound form of IL-15 and human 4-1BBL (K562-mb15-41BBL) kindly provided by Dr. Dario Campana of University of Tennessee College of Medicine (17) in RPMI1640 containing 10% fetal bovine serum (FBS), 50 U/mL penicillin, 50 μg/mL streptomycin and 100 IU/mL IL-2 for 14 d. The cultured NK cells were washed with RPMI1640 and then were used for the cytotoxicity assay.

Transfection of 721-221 cells with retroviral vector

An HLA class I-negative B cell line 721–221 was transfected with retrovirus vectors containing HLA-C*0301 (.221-Cw3) or HLA-C*0401 (.221-Cw4) as described previously (18). Transfectants were selected in the presence of 0.1 mg/mL neomycin and 0.1 mg/mL puromycin. The surface expression of HLA-C molecules was confirmed by flow cytometry using a mAb HLA-ABC (Immunotech, Marseille, France). A clone exhibiting the highest

level of HLA-C expression was used as a target in the cytotoxicity assay.

Cytotoxicity assay

NK cell cytotoxicity was assessed using the standard chromium release assay, as described previously (19). In blocking experiments, anti-ULBP Abs were added at 10 μg/mL to the ^{51}Cr labeled target cells and target cells were incubated at 37°C for 30 min before the addition of NK cells. The percentage of specific lysis was calculated using the formula: 100 × (count per minute [cpm] released from test sample-cpm spontaneous release)/(cpm maximum release − cpm spontaneous release).

Statistical analysis

The significance of difference in the PB $CD16^+CD56^-$ cell count between CBT recipients and recipients of BM, PBSCT, or healthy individual was assessed by Student's *t*-test. The significance of difference in the time of sampling after SCT between CBT, BMT and PBSCT was assessed by Mann-Whitney test. *P*-values < 0.05 were considered to be significant.

Results

An increase in the number of $CD16^+CD56^-$ NK cells in a CBT recipient

A 56-yr-old male (Patient 1) who relapsed with AML M0 after PBSCT from a sibling donor underwent CBT following preconditioning with fludarabin 125 mg/m^2, melphalan 80 mg/m^2, and 4 Gy TBI. The patient's leukemia was refractory to chemotherapy and there were 18% leukemic blasts in the PB at the time of preconditioning. He achieved complete chimerism in PB on day 22 after CBT. The WT1 copy number in BM RNA decreased from 13 000 copies/μg RNA before the start of preconditioning to 140 copies/μg RNA on day 60 (20). However, it rose to 1500 copies/μg RNA on day 80 after CBT. Although a molecular relapse was suspected, the WT1 copy number spontaneously decreased to 230 on day 172. Surface phenotype analysis of PB leukocytes on day 84 showed an increase in the count of $CD3^-CD16^+CD56^-$ NK cells (Fig. 1). The $CD16^+CD56^-$ NK cell count remained as high as 3.2–4.5 × 10^9/L for the following 11 months during which he remained in remission. The patient eventually relapsed with AML and died 16 months after CBT. The unexpected long term remission after reduced-intensity CBT associated with an increase in the $CD16^+CD56^-$ NK cell count prompted the characterization of the $CD16^+CD56^-$ NK cells of this patient and other patients who underwent allogeneic SCT.

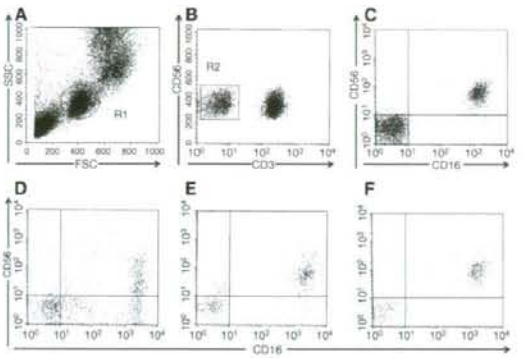

Figure 1 Phenotype of the $CD16^+$ NK cells in the peripheral blood. Representative results of flow cytometry on $CD3^-$ lymphocytes from SCT recipients and healthy individuals are shown. Gates were set up to exclude any $CD3^+$ lymphocytes as shown in (A) and (B); (C) a healthy individual; (D) a CBT recipient (Patient 1); (E) a BMT recipient; (F) a PBSCT recipient.

$CD16^+CD56^-$ NK cells in PB of allogeneic SCT recipients

Because the presence of $CD16^+CD56^-$ NK cells has been reported to be characteristics of CB, the proportion of PB $CD16^+CD56^-$ NK cells as well as their absolute count was determined for other recipients of CB and the other stem cell grafts. An increase in the $CD16^+CD56^-$ NK cell count greater than 0.5 × 10^9/L was seen in seven of 11 CBT recipients but in none of 13 BMT and eight PBSCT recipients (Figs 1 and 2). There was no significant difference in the time of sampling after SCT between CBT recipients and BMT recipients ($P > 0.772$) or CBT recipients and PBSCT recipients ($P > 0.265$). Both the $CD16^+CD56^-$ NK cell proportion and the absolute count were significantly higher in CBT recipients than in other SCT recipients or in healthy individuals. In contrast, there were no significant differences in the count of other NK cell subsets including $CD56^{dim}CD16^+$ and $CD56^{bright}CD16^-$ cells among these three SCT recipient groups (data not shown). A $CD16^+CD56^-$ NK cell increase greater than 1.5 × 10^9/L was restricted to Patient 1 and another CBT recipient with NHL (Patient 2). The $CD16^+CD56^-$ NK cell counts of Patient 2, 5 months and 15 months after CBT were 1.5 × 10^9/L and 1.8 × 10^9/L, respectively.

Surface phenotype of $CD16^+CD56^-$ NK cells and leukemic cells

To characterize this unusual NK cell subset, the surface phenotype was compared between $CD16^+CD56^-$ and $CD16^+CD56^+$ NK cells from Patient 1 and Patient 2

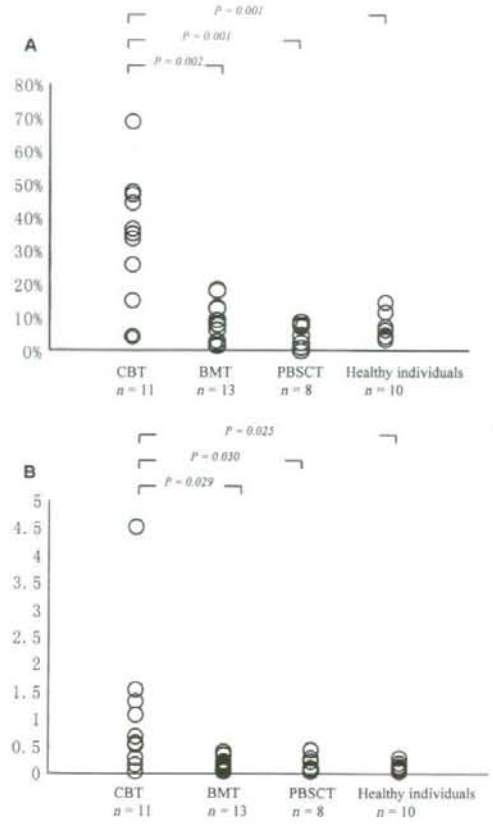

Figure 2 The proportion (A) and the absolute count (B) of $CD3^-CD16^+CD56^-$ in the PB of SCT recipients and healthy individuals. An increase in the proportion of $CD3^-CD16^+CD56^-$ NK cells (20% or more) in the PB $CD16^+$ NK cells and an increase in the absolute count of the same NK cell subset ($>0.5 \times 10^9$/L) were observed in seven of 11 CBT recipients, but in none of allogeneic 13 BM and eight PBSC transplant recipients. The $CD3^-CD16^+CD56^-$ cell count was calculated by multiplying the WBC count with the proportion (%) of this subset among the total cell event.

(Table 1). All $CD16^+CD56^-$ cells, similarly to $CD16^+CD56^+$ cells, expressed CD11a, CD18, but did not express a B-cell marker CD19, or the myeloid marker CD33 (data not shown). There were no differences in the expression levels of two major inhibitory NK receptors CD158a and CD158b between the two NK cell subsets (data not shown). On the other hand, the proportions of cells expressing activating NK receptors including NKG2D in $CD16^+CD56^-$ NK cells tended to be lower than those of $CD16^+CD56^+$ NK cells.

The leukemic cells obtained from Patient 1 before CBT exhibited an NKG2D ligand ULBP2 (Fig. 3). When the leukemic cells obtained after relapse was examined, the ULBP2 expression was observed to have decreased to levels comparable to ULBP1 and ULBP3.

Phenotypic change of $CD16^+CD56^-$ NK cells after *in vitro* culture

$CD16^+CD56^-$ NK cells derived from CB are reported to undergo differentiation *in vitro* in the presence of IL-2 (15, 21) and are therefore thought to be precursors of $CD16^+CD56^+$ NK cells (15). $CD16^+CD56^-$ NK cells were enriched from PBMCs of Patient 1 and Patient 2 and cultured in the presence of 100 IU/ml of IL-2 with or without irradiated K562-mb15-41BBL. In accordance with the results of previous studies, $CD16^+CD56^-$ NK cells from Patient 1 became $CD16^+CD56^+$ after *in vitro* culture (Fig. 4). Cultured $CD16^+CD56^-$ NK showed a tendency toward an increased expression of activating receptors including NKp30, NKp44, NKp46 and NKG2D, but did not show any changes in the expression of inhibitory receptors including CD158a, CD158b and NKG2A (Table 1).

Specificity of cultured $CD16^+CD56^-$ NK cells

Although attaining molecular remission in association with an increase in the $CD16^+CD56^-$ NK cells suggests the involvement of these NK cells in the GVL effect,

Table 1 Phenotype of the NK cell subsets from two CBT recipients

			NKp30		NKp44		NKp46		NKG2D	
			%	MFI	%	MFI	%	MFI	%	MFI
Patient 1	$CD56^+CD16^+$	Fresh	3.7	11.5	0	7.51	56.7	37.9	61.0	35.6
		Cultured	43.1	33.2	71.2	88.9	61.3	48.1	100.0	156.0
	$CD56^+CD16^-$	Fresh	0.0	8.37	0.0	7.57	17.6	12.6	46.7	12.6
		Cultured	14.2	10.4	51.4	31.0	54.2	26.8	99.9	26.8
Patient 2	$CD56^+CD16^+$	Fresh	3.6	6.71	0.0	7.72	42.9	44.3	72.3	44.3
		Cultured	14.2	39.4	51.4	49.4	54.2	54.4	99.5	54.4
	$CD56^+CD16^-$	Fresh	0.0	8.65	0.0	8.31	21.5	16.9	69.0	16.9
		Cultured	58.1	47.6	66.3	51.4	75.2	64.8	98.5	64.8

$CD16^+CD56^-$ and $CD16^+CD56^-$ NK cells were isolated from two CBT recipients and cultured with irradiated K562-mb15-41BBL in the presence of IL-2 for 14 d. Cultured NK showed increased expression of activating NK receptors including NKp30, NKp44, NKp46 and NKG2D.

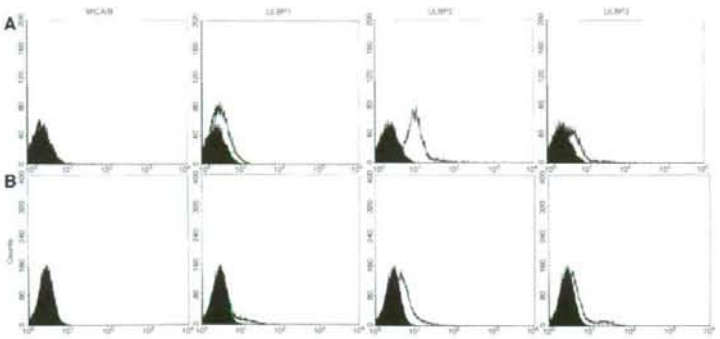

Figure 3 Expression of NKG2D ligands on leukemic cells from Patient 1. (A) leukemic cells obtained before CBT; (B) leukemic cells obtained after relapse. The proportion of ULBP2 expressing leukemic cells decreased from 59% to 9%.

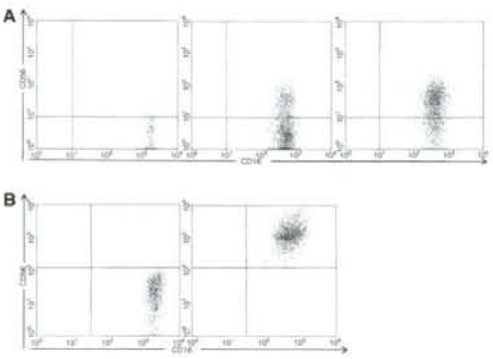

Figure 4 Phenotypic change of CD16⁺CD56⁻ NK cells with time associated with *in vitro* culture. Isolated CD16⁺CD56⁻ cells from Patient 1 were cultured in the presence of 100 IU/L IL-2 without (A) or with K562-mb15-41BBL (B). CD16⁺CD56⁻ NK cells from CBT recipients became CD16⁺CD56⁺ after the *in vitro* culture.

there was no killer-cell immunoglobulin receptor (KIR)-ligand (KIR-L) mismatch between Patient 1 and the CB donor; Patient 1 and the CB donor shared C*0102 and C*0304. To determine whether cultured NK cells derived from CD16⁺CD56⁻ NK cells retain specificity restricted by KIR-L of target cells, cultured NK cells from Patient 1 and Patient 2 who possessed C*0102 and C*1202 were separated into CD158b⁺ and CD158b⁻ NK cells, and were examined for their cytotoxicity against 721–221 cells transfected with different HLA-C alleles (Fig. 5). CD158b⁺ NK cells failed to kill 721–221 cells transfected with HLA-C*0301 (.221-Cw3) while they killed both wild-type 721–221 cells and 721–221 cells transfected with HLA-C*0401 (.221-Cw4). Conversely, CD158b⁻ NK cells not only killed 721–221 cells but they also killed .221-Cw3 and .221-Cw4 cells, thus indicating that the cytotoxicity due to the cultured CD158b⁺ NK cells is inhibited by the KIR-L Cw3 of the target cells.

Cytotoxicity of cultured CD16⁺CD56⁻ NK cells against leukemic cells

When leukemic cells obtained from Patient 1 before CBT were used as a target, both CD158b⁺ and CD158b⁻ NK cells showed similar cytotoxicity to that of unfractionated NK cells (Fig. 6). The cytotoxicity was blocked by

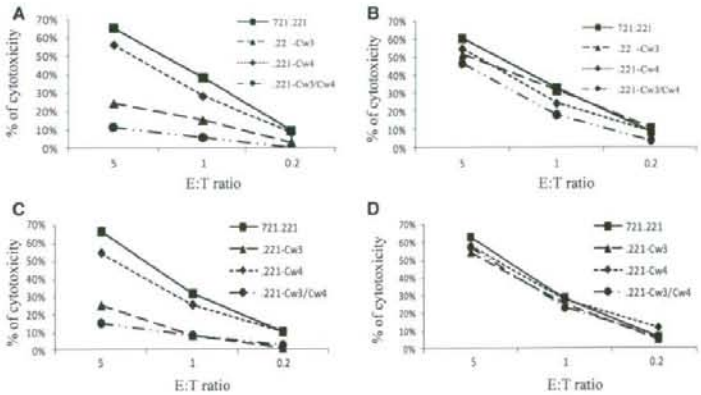

Figure 5 Specificity of NK cells derived from CD16⁺CD56⁻ NK cells. Cultured NK cells derived from CD16⁺CD56⁻ cells of Patient 1 (A and B) and Patient 2 (C and D) were separated into CD158b⁺ (A and C) and CD158b⁻ cells (B and D) and were examined for the cytotoxicity against 721-221 cells and 721-221 transfected with different HLA-C alleles C*0301 (.221-Cw3) and C*0401 (.221-Cw4). The data represent one of two experiments which produced similar results.

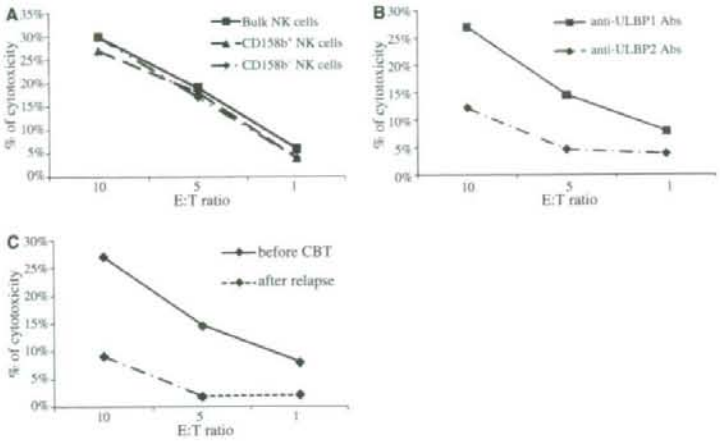

Figure 6 Cytotoxicity of cultured NK cells against leukemic cells. (A) Unseparated and separated NK cells were tested against leukemic cells obtained before CBT; (B) Leukemic cells were incubated in the presence of anti-ULBP1 or ULBP2 Abs before incubation with cultured NK cells; (C) Cytotoxicity of unseparated NK cells were tested against leukemic cells obtained before CBT or after relapse. The data represent one of three experiments which produced similar results.

treatment of leukemia cells with anti-ULPB2 mAbs. Leukemic cells obtained after relapse were relatively resistant to killing by cultured NK cells in comparison to those obtained before CBT.

Discussion

The present study revealed an increase in a unique NK cell subset characterized by CD16$^+$CD56$^-$ in CBT recipients. Although CD3$^-$CD16$^+$CD56$^-$ cells comprise monocytes, an increase in this subset was due to an increase in immature NK cells because they did not express a myeloid marker CD33 and acquired CD56 expression by *in vitro* culture in the presence of IL-2. An increase in NK cells with a similar phenotype has been shown in patients with solid tumors who were treated with IL-2 (21) and in those with HIV infection (22). Our CBT recipients did not receive cytokine therapy nor show any signs of viral infections at sampling. The expression of KIRs including CD158a and CD158b was not depressed in CD16$^+$CD56$^-$ cells of Patient 1 and Patient 2 in contrast to those of HIV patients (22). An *in vitro* culture of CD16$^+$CD56$^-$ NK cells from patients with HIV viremia in the presence IL-2 reportedly failed to induce NKp44 expression while it did induce the NKp44 expression by CD16$^+$CD56$^-$ NK cells from the two CBT recipients. It is therefore unlikely that the increase in the CD16$^+$CD56$^-$ cell count in the CBT recipients was secondary to viral infections.

Gaddy *et al.* demonstrated a novel subset of NK cells characterized by a phenotype CD16$^+$CD56$^-$ to exist in CB (12). They hypothesized that this NK cell subset represents immature NK cells capable of differentiating into CD16$^+$CD56$^+$ NK cells (15). CD16$^+$CD56$^-$ cells of our patients also underwent differentiation into CD16$^+$CD56$^+$ cells when they were cultured in the presence of IL-2. Therefore, CD16$^+$CD56$^-$ cells in PB after CBT may be derived from immature NK cells or NK precursor cells which existed in CB grafts. Previous studies on NK cells from SCT recipients and *ex vivo* engineered CB NK cells did not reveal an increased proportion of CD16$^+$CD56$^-$ cells (23–25). Both Patient 1 and Patient 2 received an HLA-mismatched CB graft although there was no KIR-L mismatch. Notably, Patient 1 had a large leukemic burden at the time of reduced-intensity preconditioning. It is therefore plausible that residual leukemic cells may have stimulated NK cell precursors to recruit CD16$^+$CD56$^-$ NK cells in Patient 1.

Patient 1's leukemic cells obtained before CBT expressed ULBP2. The incubation of CD16$^+$CD56$^-$ NK cells derived from Patient 1 in the presence of IL-2 and the K562 transfectant augmented NKG2D expression and the cultured NK cells showed cytotoxicity against leukemic cells despite that cultured NK cells retained KIR-L specificity and Patient 1's leukemic cells expressed matched KIR-L HLA-C*0304/C*0102. The cytotoxicity by the cultured NK cells decreased against leukemic cells treated with anti-ULBP2 Abs, and also against the leukemic cells obtained from Patient 1 after relapse which were devoid of ULBP2 expression. These findings suggest that mature NK cells derived from CD16$^+$CD56$^-$ NK cells may have exerted GVL effect on Patient 1's leukemic cells by way of interaction of NKG2D and ULBP2. The aberrant expression of NKG2D ligands by leukemic cells has been demonstrated by previous studies (26), but its influence on the outcome of allogeneic SCT has not yet been clarified. The results of the present study